Comparative genomics reveals the origin of fungal hyphae and multicellularity

Enikő Kiss[1,2], Botond Hegedüs[1], Torda Varga[1], Zsolt Merényi[1], Tamás Kószó[1], Balázs Bálint[1], Arun N. Prasanna[1&], Krisztina Krizsán[1], Meritxell Riquelme[3], Norio Takeshita[4], László G. Nagy[1*]

[1]Synthetic and Systems Biology Unit, Institute of Biochemistry, BRC-HAS, 6726 Szeged, Hungary
[2]University of Szeged, Faculty of Science and Informatics, 6720, Szeged, Hungary
[3]Department of Microbiology, Centro de Investigación Científica y de Educación Superior de Ensenada, 22860 Ensenada, Baja California, Mexico
[4]Microbiology Research Center for Sustainability (MiCS), Faculty of Life and Environmental Sciences, University of Tsukuba, 305-8572, Japan

*Author for correspondence: lnagy@fungenomelab.com
&Current address: Red Sea Science and Engineering Research Center, 4700 King Abdullah University of Science and Technology (KAUST), Thuwal 23955-6900, Kingdom of Saudi Arabia

Abstract

Hyphae represent a hallmark structure of multicellular fungi with immense importance in their life cycle, including foraging for nutrients, reproduction, or virulence. Hypha morphogenesis has been the subject to intense interest, yet, the origins and genetic underpinning of the evolution of hyphae are hardly known. Using comparative genomics, we here show that the emergence of hyphae correlates with multiple types of genetic changes, including alterations of gene structure, gene family diversification as well as co-option and exaptation of ancient eukaryotic genes (e.g. phagocytosis-related genes). Half of the gene families involved in hypha morphogenesis have homologs in unicellular fungi and non-fungal eukaryotes and show little or no duplications coincident with the origin of multicellular hyphae. Considerable gene family diversification was observed only in transcriptional regulators and genes related to cell wall synthesis and modification. Despite losing 35-46% of their genes, yeasts retained significantly more multicellularity-related genes than expected by chance. We identified 414 gene families that evolved in a correlated fashion with hyphal multicellularity and may have contributed to its evolution. Contrary to most multicellular lineages, the origin of hyphae did not correlate with the expansion of gene families encoding kinases, receptors or adhesive proteins. Our analyses suggest that fungi took a unique route to multicellularity that involved limited gene family diversification and extensive co-option of ancient eukaryotic genes.

Introduction

The evolution of multicellularity (MC) is considered one of the major transitions in the history of life[1]. It evolved in several pro- and eukaryote lineages[2–7], each representing a unique solution to the challenges of multicellular organization[6]. Among the eukaryotes, two major modes for acquiring multicellularity are the clonal and aggregative routes[5,6,8–10], which differ in how multi-celled precursors emerged by adhesion, cooperation, communication and functional diversification of cells[3,11,12].

Fungi represent one of the three kingdoms where multicellular forms dominate among extant species[13], yet, our knowledge on the evolutionary origin of multicellularity in this group is very incomplete. While most multicellular lineages can be recognized as either clonal or aggregative by comparisons to their unicellular relatives, fungal multicellularity has been recalcitrant to such categorization[6,14]. The thalli of fungi are made up of hyphae, thin, tubular structures that grow by apical extension to form a mycelium that explores and invades the substrate. Hyphal multicellularity has a number of unique properties compared to clonal and aggregative multicellularity, raising the possibility that its evolution follows markedly different principles[7]. First, hyphae might have evolved by the gradual elongation of substrate-anchoring rhizoids of early fungi[15–18], through multinucleate intermediates, in contrast to clonal and aggregative lineages, where the first multi-celled clusters probably emerged via related cells sticking together (e.g. choanoflagellates[19]), or gathering to form a syncytial body (e.g. *Capsaspora*)[9]. Because early hyphae were uncompartmentarized, their evolution could have bypassed the need to resolve group conflicts and align the fitness of individual cells[7]. Alternatively, it is possible that conflicts are resolved at the level of individual nuclei[20]. Second, hyphae maximize foraging and nutrient assimilation efficiency and minimize competition for nutrients by a fractal-like growth mode[16,21,22]. This mode of origin differs from that of other multicellular lineages where selection for increased size possibly helped avoiding predation[2]. Hyphae might have also facilitated the transition of fungi to terrestrial life[23] and confer immense medical relevance to pathogenic fungi[24]. Hyphae of extant fungi rarely stick to each other in vegetative mycelia and adhesion becomes key only in fruiting bodies[25–27] - which, in terms of complexity level, resemble complex multicellular metazoans and plants[7,28] - or in the attachment to host surfaces[29]. Thus, whereas in most multicellular lineages adhesion, cell-cell cooperation, communication and differentiation represent the main hurdles to the emergence of multicellular precursors[3,6,30–32], fungi might have had different obstacles to overcome.

While the origins of hyphae are poorly known, information on the molecular and cellular basis of hyphal morphogenesis is abundant (for recent reviews see refs[33–38]), permitting evolutionary genomic analyses of the origins of hyphae. Hyphal morphogenesis builds on cell polarization networks[39], the exo- and endocytotic machinery[40], long range vesicle transport as well as fungal-specific traits such as cell wall synthesis and assembly[41], and the selection of branching points and sites of septation[42], among others. A key structure of hyphal growth is the Spitzenkörper[43], which acts as a distribution center for vesicles transporting cell wall materials and various factors to the hyphal tip. The cytoplasmic microtubule network provides the connection between vesicle cargo through the ER and Golgi and the Spitzenkörper, from where

2

83   vesicles move along actin microfilaments to the hyphal tip and secrete their content to deposit
84   new cell wall components and provide surface expansion. Further key processes include the
85   recycling of excess membrane in the subapical zone, the activation of cAMP pathways and
86   mitogen activated protein kinase (MAPK) cascades and finally the transcriptional control of
87   morphogenesis (for detailed reviews see refs[44–49]).
88
89   A complex hyphal thallus has been reported from a 407 million year old fossil
90   Blastocladiomycota[51], whereas Glomeromycotina-like hyphae and spores were preserved 460
91   million years ago[50,52] indicating that hyphal growth dates back to at least the Ordovician. Most
92   Dikarya and Mucoromycota grow true hyphae, whereas a significant diversity of forms is found
93   in the early diverging Blastocladiomycota, Chytridiomycota and to a smaller extent the
94   Zoopagomycota. The Chytridiomycota is dominated by unicellular forms that anchor themselves
95   to the substrate by branched, root-like rhizoids[16,50] which have been hypothesized as the
96   precursors to hyphae[15,53]. An alternative hypothesis designates hypha-like connections in the
97   thalli of polycentric chytrid fungi (e.g. *Physocladia*) as intermediates to true hyphae[17]. Like
98   chytrids, most Blastocladiomycota form mono- or polycentric, unicellular thalli, although some
99   species form wide, apically growing structures resembling true hyphae (e.g. *Allomyces*) or
100   narrow exit tubes on zoosporangia (e.g. *Catenaria* spp.)[16,50,54]. In spite of these intermediate
101   forms, the unicellular dominance in these phyla aligns well with a unicellular ancestry and
102   potential convergent origins of hypha-like structures[17].
103
104   Here we examine the evolution of hyphal multicellularity in fungi by reconstructing
105   historical patterns of known hyphal morphogenesis genes as well as by systematic searches of
106   fungal genomes for gene families whose evolution correlates with that of hyphae. We analyze
107   the genomes of 4 plesiomorphically unicellular, 40 hyphal (one of which is ambiguous) and 14
108   secondarily simplified (yeast-like) fungi as well as 13 non-fungal relatives. Given the likely
109   convergent origins of hyphae, we focus our analyses on multiple nodes of the fungal tree to
110   where origin(s) of hyphal growth can be localized with confidence. Our analyses reveal a deep
111   eukaryotic origin of most morphogenesis-related families, limited gene family diversification in
112   correlation with the emergence of hyphal MC and that secondarily simplified yeast-like fungi
113   retained most of the genes for multicellular growth.

Results and discussion

Hyphae evolved in early fungal ancestors

116   To understand the origin of hyphae, we constructed a species phylogeny representing 71
117   species (Supplementary Table 1) by maximum likelihood analysis of a supermatrix of 595
118   single-copy orthologs (175,535 characters Fig. 1a).
119
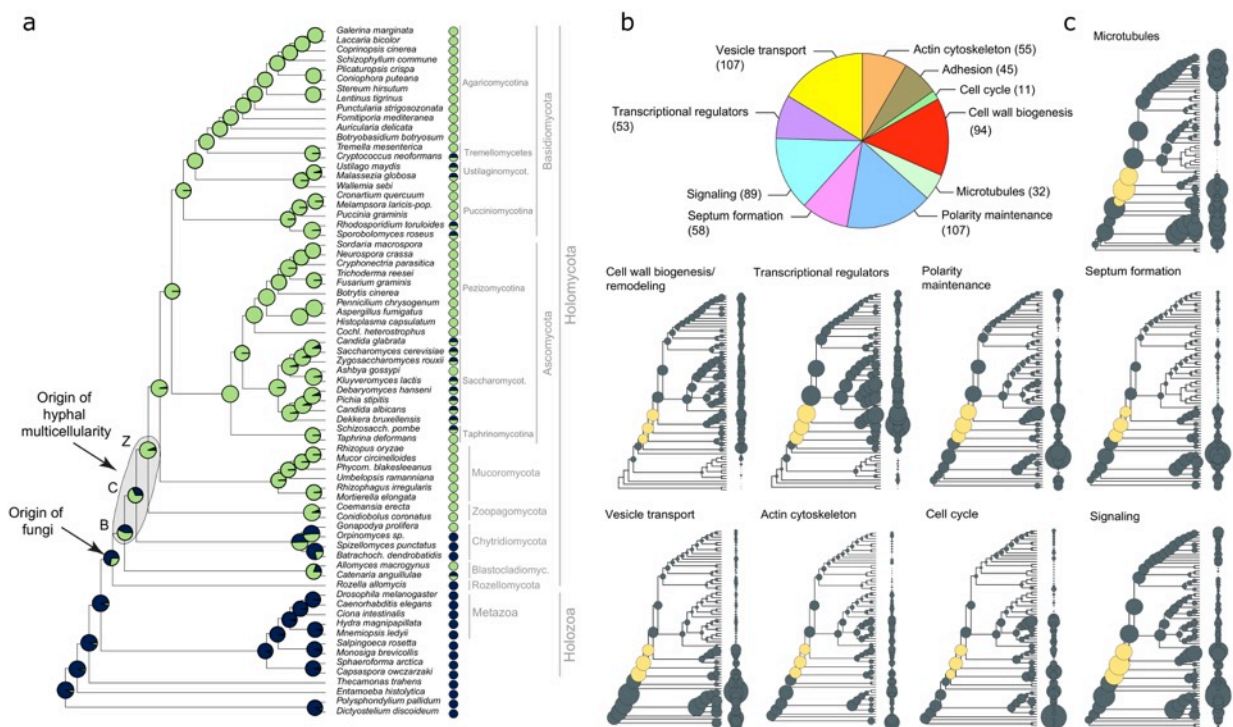
Fig. 1. The evolution of hyphal multicellularity and underlying genes in fungi. (a) Phylogenetic relationships among 71 species analyzed in this study. Pie charts at nodes show the proportional likelihoods of hyphal (green) and non-hyphal (dark blue) ancestral states reconstructed using Bayesian MCMC. Character state coding of extant species used in ancestral state reconstructions is shown next to species names. BCZ nodes: origin of hyphal growth could be assigned with confidence are highlighted (note the uncertainty imposed by filamentous Blastocladiomycota). (b) the distribution of literature-collected hypha morphogenesis genes among 10 main functional categories. (c) Ancestral reconstructions of gene copy number in 9 main hypha morphogenesis-related categories of genes (see Fig. 5c for adhesion). Bubble size is proportional to reconstructed ancestral gene copy number. BCZ nodes are shown in yellow.

Our species phylogeny recapitulates recent genome-based phylogenies of fungi[55–58], with the Rozellomycota, Blastocladiomycota and the Chytridiomycota splitting first, second and third off of the beckbone, respectively (ML bootstrap: 100%). We performed ancestral character state reconstruction using Bayesian MCMC to identify the putative origin of hyphal growth. This supported an emergence of hyphae from unicellular ancestors in basal fungi. The distribution of posterior probability values indicated three nodes as the most likely origins of hyphal multicellularity, which represent the split of Blastocladiomycota, Chytridiomycota and Zoopagomycota lineages, referred hereafter to as BCZ nodes. The posterior probability for the hyphal state started to rise in the most recent common ancestor (MRCA) of the Blastocladiomycota and higher fungi (PP: 0.53, Fig. 1a) and increased to 0.68 and 0.92 in the next two nodes along the backbone of the tree. This suggests that hyphae evolved either in one of the BCZ nodes or it may have been a gradual process unfolding in these three nodes. This uncertainty likely reflects diverse hypha-like morphologies in the Blastocladio- and Chytridiomycota and is consistent with the convergent origins of hypha-like morphologies[7,17,18].

146   To account for this uncertainty, we focus on BCZ nodes in subsequent analyses of hypha
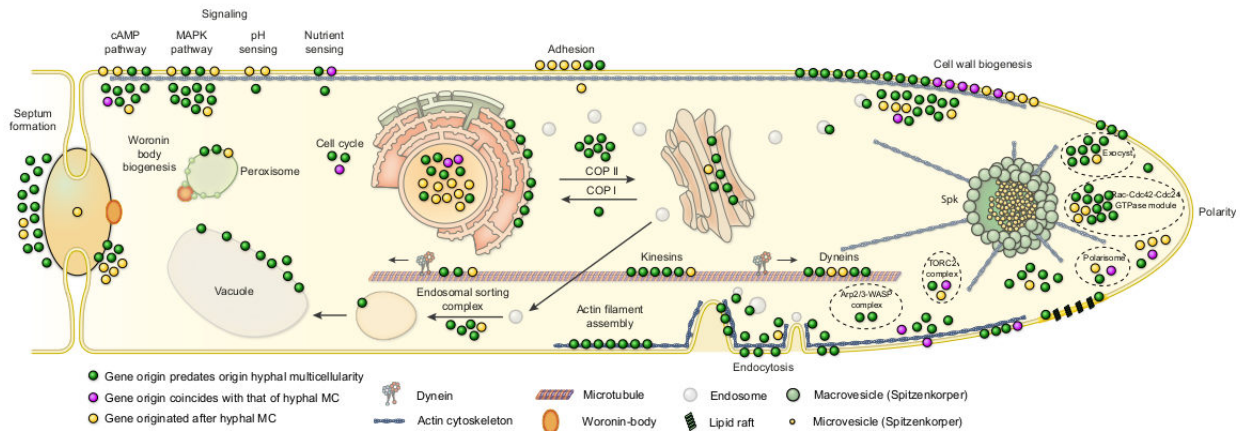147   morphogenesis genes.
148

The evolution of hypha morphogenesis genes

150   Our survey of the literature for hyphal multicellularity-related genes yielded 651 genes (from 519
151   publications), mostly from well-studied model systems such as *A. fumigatus, A. nidulans*, *N.*
152   *crassa, S. cerevisiae* and *C. albicans* (Supplementary Table 2). We categorized genes
153   according to the broader function they fulfill in hyphal growth into nine functional groups: actin
154   cytoskeleton regulation, polarity maintenance, cell wall biogenesis/remodelling, septation
155   (including septal plugging), signaling, transcriptional regulation, vesicle transport, microtubule-
156   based transport and cell cycle regulation. The categories "polarity maintenance" and "vesicle
157   transport" contained the largest number of genes (107 in each), whereas "cell cycle regulation"
158   contained the fewest (11) (Fig.1b). The collected genes grouped into 362 families by Markov
159   clustering of the a 71-genome dataset.
160

161   Reconstructions of gene duplication/loss histories for nine functional categories of hypha
162   morphogenesis gene families are shown on Fig. 1c. A general pattern that emerges from these
163   is that the origin of many gene families (181 families, 50%) predate that of hyphal MC (Fig. 2,
164   Supplementary Fig. 1), indicating that fungi have co-opted several conserved eukaryotic
165   functionalities for hyphal growth. A significant proportion of multicellularity-related gene families
166   (164 families, 45.3%) emerged after the origin of hyphal MC, indicating lineage- and species-
167   specific genetic innovations. Only 17 families (4.7%) originated in BCZ nodes and were
168   conserved thereafter (Table 1), providing potential candidates that shaped the evolution of
169   hyphal MC. These include two families of transcriptional regulators (encoding StuA and MedA
170   proteins in *A. fumigatus*)[59,60], six related to cell wall biogenesis, three to actin cytoskeleton
171   regulation, three to polarity maintenance, two families involved in signaling and one involved in
172   cell cycle regulation. One of the families contains the *S. cerevisiae* Pan1, an endocytic adaptor
173   protein at the plasma membrane. Pan1 triggers the recruitment of the Arp2/3 complex to the site
174   of endocytosis, which is necessary for the recycling of excess membrane in the subapical region
175   during hyphal growth[40]. Another example is the polarisome component BNI-1 from *N. crassa*.
176   Knockout studies showed that it mediates actin cable assembly in filamentous fungi and has a
177   role in diverse morphogenesis-related processes[61]. Other proteins involved in establishing cell
178   polarity are the Bem1 actin cytoskeleton reorganizing factor[62,63] and the Rax1, associated with
179   bipolar budding in *S. cerevisiae*[64].

180
181 Fig. 2. Phylogenetic age distribution of hypha morphogenesis genes. Schematic outline of terminal hyphal
182 cell is shown with genes marked by dots and colored by phylogenetic age. Genes whose origin predates
183 that of hyphal multicellularity (green, 72,2%) dominate the hyphal morphogenetic machinery, followed by
184 genes that originated after hyphal MC (yellow, 21,2%) and genes whose origin approximately coincides
185 with that of hyphae (purple, 6,6%). Data based on only *A.fumigatus* orthologs. See also Supplementary
186 Figure 1 for gene names.
187

Emergence of gene family	*A. fumigatus* ortholog	*S. cerevisiae* ortholog	functional category	cluster ID
lca of Dikarya, Mucoromycota, Zoopagomycota, Chytridiomycota, Blastocladiomycota	Afu7g03870	PAN1/YIR006C	actin cytoskeleton	4903
	crh3/Afu3g09250	UTR2/YEL040W	cell wall biogenesis	374
	gel7/Afu6g12410	GAS1/YMR307W	cell wall biogenesis	435
	Afu6g04940	BNR1/YIL159W	polarity establishment	3689
	Afu4g04120	BEM1/YBR200W	polarity establishment	2482
	stuA/Afu2g07900	PHD1/YKL043W	transcriptional regulation	2479
	medA/Afu2g13260	NA	transcriptional regulation	8521
lca of Dikarya, Mucoromycota, Zoopagomycota, Chytridiomycota	Afu6g07910	SLM1/YIL105C	actin cytoskeleton	1561
	Afu8g04520	SLA1/YBL007C	actin cytoskeleton	5953
	Afu4g06130	WHI2/YOR043W	cell cycle regulation	2915
	Afu4g00620	DFG5/YMR238W	cell wall biogenesis	843
	Afu8g02320	NA	cell wall biogenesis	3398
	chsD/Afu1g12600	NA	cell wall biogenesis	9065
	rgsB/Afu4g12640	RAX1/YOR301W	polarity establishment	2900
	Afu2g08800	SSY1/YDR160W	signaling	49
	ricA/Afu4g08820	NA	signaling	5950
lca of Dikarya, Mucoromycota, Zoopagomycota	kre6/Afu2g11870	KRE6/YPR159W	cell wall biogenesis	293

188 Table 1: List of the 17 gene families whose emergence shows correlation with the evolution of hyphal MC
189 based on COMPARE analysis.
190
191   Gene families related to septation, polarity maintenance, cell cycle control, vesicle
192 transport and microtubule-based transport are generally more diverse in animals, non-fungal
193 eukaryotes and their ancestors than in fungi, suggesting that despite the key role of these

6

194   families in hyphal MC, they evolved primarily by gene loss in fungi (Fig 1c). Cell wall synthesis
195   and remodeling as well as transcription regulation related families, on the other hand, show
196   expansions in MC fungi, suggesting that the diversification of these gene families could have
197   played roles in the evolution of hyphal MC (Fig 1c).

198

199   Ninety-three (25.7%) of the 362 hyphal morphogenesis-related gene families showed
200   duplications in BCZ nodes (Supplementary Table 3). Enrichment analysis of gene duplications
201   revealed no individual gene families with significantly increased number of duplications
202   (Benjamini-Hochberg corrected P<0.05, Fisher's exact test) in BCZ nodes, relative to the rest of
203   the tree (Supplementary Table 4). The same analysis on the 9 functional groups showed
204   significantly increased numbers of duplications in the cell wall biogenesis and transcriptional
205   regulation categories. These analyses suggest that the evolution of hyphal growth in BCZ nodes
206   did not generally coincide with a period of extensive gene duplication except in cell wall
207   biogenesis and transcriptional regulation-related gene families. Collectively, reconstructions of
208   gene family evolution revealed the lack of a major burst of gene family origin or that of
209   duplications coincident with the evolution of hyphal MC.

210

211   We analyzed whether changes in basic structural properties of genes show a correlation
212   with the evolution of hyphal MC. Significant differences (P < 0.05) were observed in gene, CDS
213   and intron lengths between unicellular and multicellular fungi (Supplementary Fig. 2,
214   Supplementary Table 5). CDS lengths of septation and polarity maintenance genes were
215   significantly higher in multicellular than in unicellular fungi (P=0.0012-0.00017, Supplementary
216   Fig. 2). An opposite pattern was observed in intron lengths, which were on average longer in
217   unicellular fungi in actin cytoskeleton, cell wall biogenesis, polarity maintenance, septation and
218   vesicle transport related genes. In actin cytoskeleton-related genes the CDS length and intron
219   length showed the same pattern: both of them were longer in multicellular species. Gene and
220   CDS lengths were significantly longer in unicellular than in multicellular fungi in genes encoding
221   adhesion and microtubule-based transport proteins. On the other hand, interestingly, no
222   significant changes in gene structure were detected in cell wall biogenesis and transcriptional
223   regulation-related genes, the two categories that displayed significant gene family diversification
224   in early filamentous fungi.

Phagocytosis is lost, but phagocytotic genes are retained by fungi

226 Our sets of hypha morphogenesis genes included several entries associated with phagocytosis
227 in non-fungal eukaryotes. This is surprising given that phagocytosis is not known in fungi and
228 their rigid cell wall forms a physical barrier to it. We therefore examined the fate of phagocytosis
229 genes in filamentous fungi based on the phagocytotic machinery of *D. discoideum*[65,66] and other
230 eukaryotes[67]. Filamentous fungi have retained several phagocytotic gene families but lost others
231 (Fig. 3). For example, members of the Arp2/3 complex, which nucleates actin filaments and
232 triggers actin cytoskeleton rearrangements[68] is conserved in filamentous fungi and is involved in
233 hyphal growth[69]. Engulfment and cell motility genes (ELMO1/2) are found in all filamentous
234 fungi, but are convergently lost in budding and fission yeasts as well as in *C. neoformans, M.*
235 *globosa* and *W. sebi*, all of which have reduced capacities for hyphal growth. The DOCK
236 (dedicator of cytokinesis) protein family, which interacts with ELMO proteins, is represented as a

237 single gene copy in filamentous fungi and yeasts. This family contains orthologs of *S. cerevisiae*
238 DCK1 (a homolog of human DOCK1), which has been shown to influence hypha
239 morphogenesis[70]. Of the broader Wiskott-Aldrich syndrome family of proteins, which reorganize
240 the actin cytoskeleton during phagocytosis, the WASP family is conserved across fungi, the
241 WAVE family is only represented in early diverging fungi and non-fungal eukaryotes, whereas
242 the WASH family has been lost in fungi, with homologs detected only in non-fungal eukaryotes,
243 consistent with recent reports[71,72]. These patterns reveal the conservation of several
244 phagocytotic genes in fungi, despite the loss of phagocytosis and the evolution of rigid cell walls
245 and osmotrophy. Previous functional analyses have shown that several of the retained genes
246 are involved in hypha morphogenesis in fungi, indicating that members of the phagocytic
247 machinery were probably exapted for hyphal multicellularity in ancient fungi.
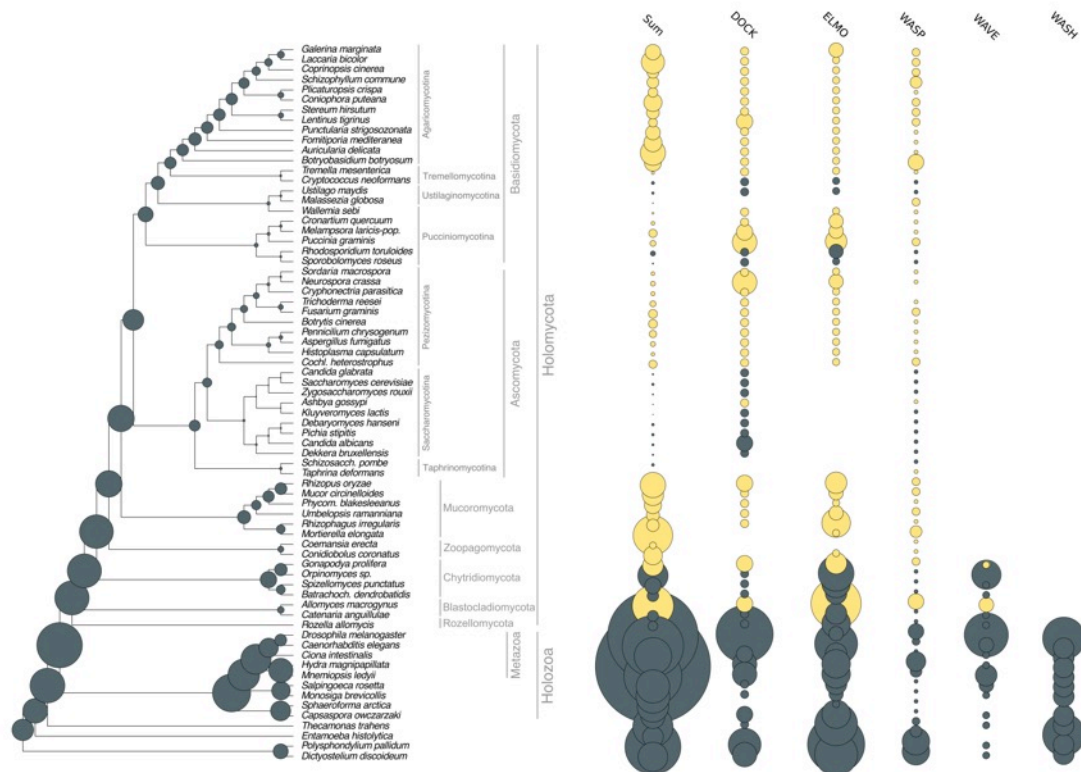
248
249 Fig. 3. Evolutionary dynamics of phagocytosis-related gene families. Several phagocytic gene families
250 retained in filamentous fungi (DOCK, ELMO, WASP). WAVE family retained only in early fungi
251 (Blastocladiomycota and Chytridiomycota), WASH family is represented only in non-fungal eukaryotes.
252 Bubble size is proportional to ancestral and extant gene copy number. Copy numbers of filamentous fungi
253 are labelled with yellow.
254

255 ## Genome-wide screen for correlated evolution between multicellularity and
256 gene family expansion

257 To identify further gene families with a potential connection to hyphal MC, we systematically
258 searched for families that show substantial dynamics in BCZ nodes. We reasoned that gene
259 families underlying hyphal MC should originate or diversify in BCZ nodes and be conserved in

8

260   descendent filamentous fungi. Searching for gene families fitting these criteria yielded 414
261   families (ANOVA, $p<0.05$, Supplementary Table 6), 114 of which originated in BCZ nodes, while
262   the others showed duplication rates that exceeded the expectation derived from genome-wide
263   collection of gene families (Fig. 4). These included several known morphogenetic families (e.g.
264   Bgt3, RgsB and Gel2 of *A. fumigatus*, Bem1 and Rax1 of *S. cerevisiae*), genes involved in actin
265   cytoskeleton and cell wall assembly, mating, pheromone response (GpaA of *A. fumigatus*),
266   sporulation and transporters, among others (Supplementary Table 6). Several of the identified
267   families contain genes with reported growth defects in *A. fumigatus* or *S. cerevisiae,* indicating
268   that our searches recovered genes relevant for hyphal MC. For example, Rax proteins are
269   major regulators of cellular morphogenesis and are involved in bud site selection in budding
270   yeasts[73,74], polarized growth in *S. pombe*[75] and polarity maintenance in filamentous fungi[76]. The
271   finding that these families originated in BCZ nodes makes them candidates for being key
272   contributors to the evolution of hyphal MC. We further detected a fungal-specific cluster of
273   tropomyosins (TPM1 in *S. cerevisiae*), which maps to the MRCA of Blastocladiomycota and
274   other fungi and comprises genes involved in polarized growth and the stabilization of actin
275   microfilaments. The family containing *S. pombe* Dip1 homologs (Afu6g12370 in *A. fumigatus*)
276   emerged in the node uniting Chytridiomycota with higher fungi and contains a single gene per
277   species afterwards, except an expansion in WGD Mucoromycota[77] and losses in the
278   Saccharomycotina. In *S. pombe*, Dip1 activates the Arp2/3 complex without preexisting actin
279   cables[78,79] and thus initiates cortical actin patch assembly and endocytosis. Because it does not
280   require pre-existing actin cables, it mediates actin cytoskeleton regulation through a mechanism
281   that seems to be specific to multicellular fungi. Finally, we detected the family containing *S.*
282   *cerevisiae* Dpp1 homologs, which shows a significant expansion (4 duplications) in BCZ nodes.
283   This family regulates morphogenetic transitions in dimorphic fungi through the synthesis of the
284   fungal signal molecule farnesol[80], which prompts us to speculate that it might have contributed
285   to the elaboration of farnesol-based communication in fungi.
286
287   Because the emergence of hyphal multicellularity overlaps significantly with that of other
288   fungal traits, it is challenging to unequivocally separate signals conferred by these traits from
289   those of hyphal MC. It is conceivable that a portion of the 414 gene families (Supplementary
290   Table 6) were detected because of signals conferred by phylogenetically co-distributed traits,
291   not necessarily multicellularity itself (see Beaulieu 2016[81] for a conceptually analogous problem
292   in analyzing taxonomic diversification). One such trait could be osmotrophy, the feeding
293   mechanism of fungi to absorb soluble goods generated by extracellular enzyme complexes[82].
294   We detected 20 gene families that showed strong correlation with hyphal MC and were
295   annotated as various transporters; such families could hypothetically be related to osmotrophy.
296   Further, among the 414 detected families, there were 84 that are currently functionally
297   uncharacterized and thus it is impossible to speculate about their role in hyphal MC.
298   Collectively, these families indicate that there are plenty of fungal genes that evolved in concert
299   with hyphal MC and that await functional characterization to establish links to hyphal MC or
300   other fungal functions.
301
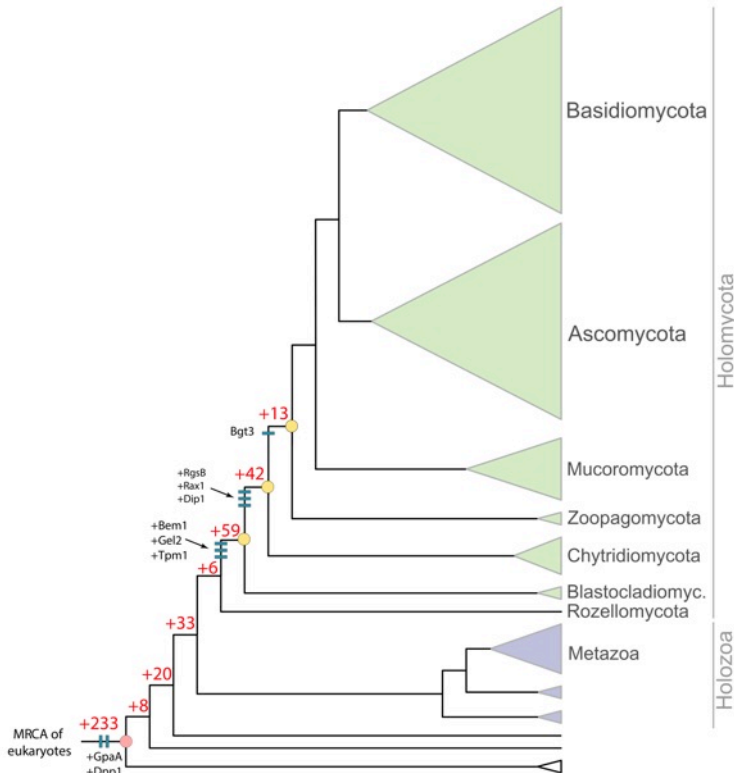
Fig. 4. Origin of 414 gene families potentially related to the evolution of hyphal MC, identified by ANOVA (p<0.05). 114 families originated in BCZ nodes, including known morphogenesis related proteins (e.g. Bgt3, RgsB, Gel2 of *A. fumigatus*, Rax1, Bem1, Tpm1 and Dpp1 from *S. cerevisiae*, Dip1 from *S. pombe*) labelled as blue bars. Red numbers at branches represent the number of gene families originated at the backbone of the species tree.

The evolution of kinase, receptor and adhesive repertoires do not correlate with hyphal multicellularity

The increased sophistication of cell-cell communication and adhesion pathways often correlates with expanded repertoires of genes encoding kinases, receptors and adhesive proteins[83–85]. We therefore, examined Ser/Thr kinase (954 clusters), hybrid histidine kinase (96 clusters), receptor (183 clusters) and adhesion (23 clusters) genes, focusing on the comparison of unicellular and filamentous fungi. Copy numbers across the 954 identified Ser/Thr kinase clusters were similar in unicellular and simple multicellular fungi, with higher kinase diversity found in complex multicellular Basidiomycota (as reported by Krizsan 2018)[86] and in *Rhizophagus irregularis* (Fig. 5a). We inferred net contractions in BCZ nodes, from 572 to 529 reconstructed ancestral kinases (81 duplications, 124 losses, Fig. 5a). Nevertheless, kinase families that duplicated here include all 3 MAPK pathways in fungi, the mating pheromone, cell wall integrity (*fus3*, *kss1*, *kdx1* from *S. cerevisiae*, *mpkB* from *A. fumigatus*) and osmoregulatory pathways (*hog1*, *ssk2*, *ssk22* from *S. cerevisiae*, *sakA*, *sskB* from *A. fumigatus*), all of which indirectly regulate hyphal growth[46–48].

Overall, fungi had fewer Ser/Thr kinases (mean 257) than metazoans (mean 643). However, the higher kinase diversity of metazoans seems to be a result of an early expansion in

325   the MRCA of Holomycota and Holozoa (Fig. 5a). While signal transduction requirements of

326   metazoan MC have been mostly discussed in the context of receptor tyrosine kinases, we found

327   no evidence for domain architectures typical of receptor tyrosine kinases in fungi. The only

328   group resembling receptor kinases is hybrid histidine kinases (HK), that comprise proteins with

329   a sensor domain, a histidine kinase domain and a C-terminal receiver domain that acts as a

330   response regulator. We inferred an expansion (24 duplications, 10 losses) of HKs in the MRCA

331   of the Chytridiomycota and other fungi, including class III and X HKs, which are linked to

332   morphogenesis[87,88]. Another wave of HK expansion was inferred in the MRCA of Mucoromycota

333   and Dikarya with 11 duplications and 4 losses (Supplementary Fig. 3).

334

335   In G-protein coupled receptors (GPCRs), an even more extreme difference was

336   observed between fungi and metazoans (Fig. 5b). A large receptor expansion was observed in

337   the latter, which resulted in 135-583 genes in extant animals. Out of the 183 analyzed GPCR

338   families, only 19 were found in fungi, and only one of them was generally conserved across

339   fungal species. This family contains STE3 and STE3-like a-factor mating pheromone receptors,

340   involved in pheromone-dependent signal transduction, cellular conjugation and cell fusion.

341

342   Adhesive cell surface proteins are key mediators of the transition to MC in colonial and

343   aggregative lineages[3,5,6], which is reflected in their higher copy numbers in multicellular

344   organisms[89]. We identified 45 families of putative adhesion-related proteins in fungi, including

345   adhesins, flocculins, hydrophobins, various lectins and glycosylphosphatidylinositol (GPI)-

346   anchored cell wall proteins. Our reconstructions of the evolution of these families (Fig. 5c)

347   revealed no expansion but a small contraction (from 17 to 14 copies) in BCZ nodes. Expansions

348   were inferred in the Agaricomycotina and in Saccharomycotina yeasts (*C. albicans, P. stipitis,*

349   *D. hansenii*). The expansion in the Agaricomycotina was driven by class1 hydrophobins and

350   homologs of the *C. neoformans* Cfl1 (an adhesive protein with roles in signaling and

351   morphogenesis regulation)[90]. Diversification of these families correlates with the evolution of

352   fruiting bodies and probably reflects the emergence of complex multicellularity[7]. The higher copy

353   numbers in yeast species relate to several yeast-specific adhesin and lectin-like cell wall

354   proteins that contain experimentally characterized adhesive proteins of human pathogenic fungi

355   (e.g. *Candida* spp.)[91,92].

356

357   Taken together, the evolution of kinase, receptor and adhesive protein repertoires

358   highlights an important difference between fungi and other multicellular lineages. We observed

359   no significant expansion of such families in filamentous fungi, whereas kinase and adhesion

360   related genes expanded in complex multicellular Agaricomycotina. This might be explained by

361   the two-step nature of the evolution of complex MC in fungi[7,93] that proceeds through an

362   intermediate complexity level, hyphal MC, as opposed to metazoans, where complex MC

363   evolved in a more direct way[14].
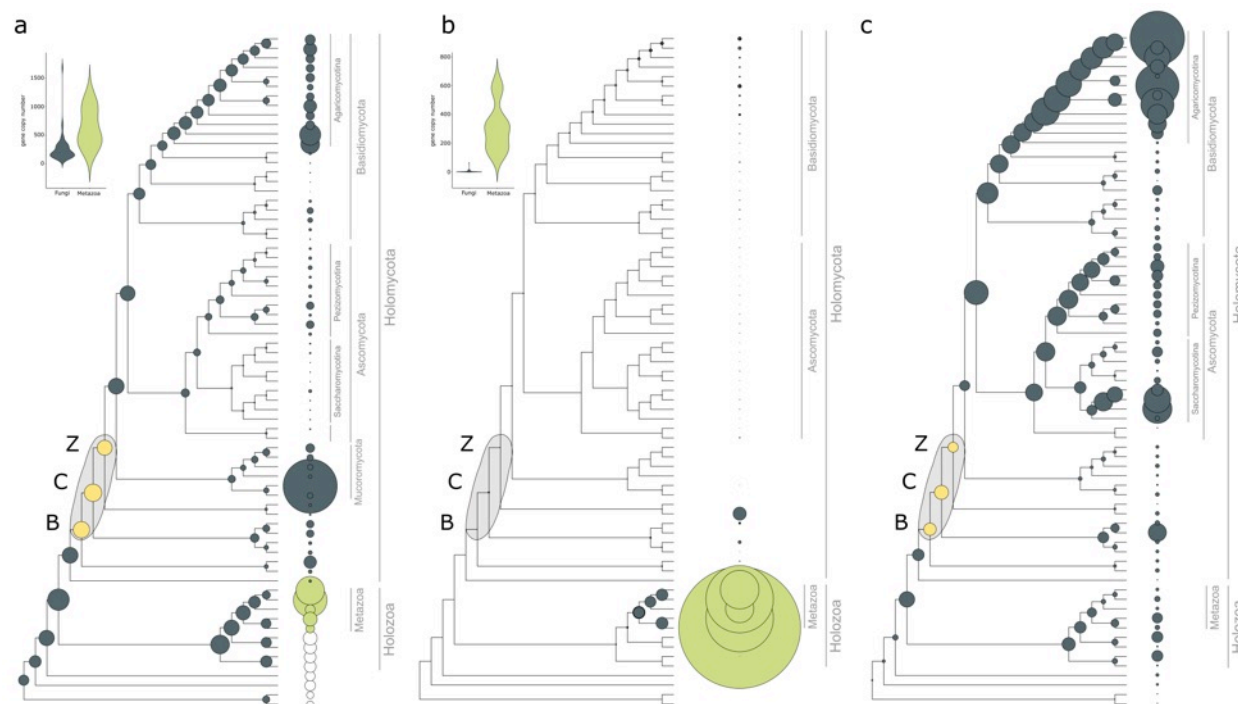
Fig. 5. Gene family evolution of Serine-Threonine kinases (a), transmembrane receptors (b) and adhesion-related genes (c). BCZ nodes (yellow) represent the putative origin of hyphal MC. Bubble size across the tree is proportional to reconstructed ancestral gene copy number and copy number of extant species (shown right to the tree). Violin plots for kinases (a) and receptors (b) show copy number distribution of gene families in multicellular fungi (grey) and metazoans (green).

Yeasts retain most genes required for hyphal morphogenesis

Yeasts are secondarily simplified organisms with reduced ability to form hyphae and that spend most of their life cycle as unicells[16,18,53,94]. Our ancestral character state reconstructions imply that yeasts derived from filamentous ancestors (Fig. 1a), and thus they represent a classic example of reduced complexity. They were hypothesized to have lost MC[95], even though rudimentary forms of hyphal growth (termed pseudohyphae) exist in most species. We scrutinized the fate of MC-related genes in five predominantly yeast-like lineages[94], the Saccharomycotina, Taphrinomycotina, Pucciniomycotina, Ustilaginomycotina and Tremellomycotina. Because yeast genomes have undergone extreme streamlining during evolution, we evaluated gene loss among MC-related genes in comparison to genome-wide figures of gene loss.

Yeast species generally have fewer MC-related genes and reconstructions indicate more losses than duplications along branches of yeast ancestors (Fig. 6). However, when we corrected for genome-wide reductions in gene number, we found that hyphal morphogenesis genes are underrepresented among lost genes compared to other functions (Fig. 6a, Supplementary Table 7). Most groups of hyphal morphogenesis genes are significantly depleted (P<0.05, Fisher's exact test) among gene losses in yeast clades (except the Ustilaginomycotina). We recovered only 6 cases where losses of MC-related genes were significantly overrepresented (P<0.05, Fisher's exact test, Supplementary Table 7), in proteins

12

390   related to adhesion and microtubule-based transport. Higher than expected loss rates in such
391   proteins were observed in the Taphrinomycotina, Pucciniomycotina, Tremellomycotina and the
392   Saccharomycotina, suggesting that microtubule-based transport and adhesion-related functions
393   become dispensable for these yeasts clades. Losses in 'microtubule system' are particularly
394   interesting from the perspective of long-range transport of vesicles and nuclei along hyphae.
395   Microtubule system-related genes with reduced repertoires in yeasts include gamma-tubulin
396   complex proteins, kinesins, dynactin, dynein heavy chain (nudA), and the dynactin linking
397   protein ro-2[96]. Of the five yeast-like clades, the budding and fission yeast lineages show the
398   most gene losses, consistent with the strongest reduction of hyphal growth abilities in these
399   clades. A similar pattern was found for NADPH oxidases, which is consistent with previous
400   reports: concurrent losses in all yeast-like clades, with complete loss of the family in the
401   Saccharomycotina, Ustilaginomycotina, in *S. pombe* and *C. neoformans* (Supplementary Fig.
402   4).
403
404   Altogether 54-65% of MC-related genes were retained in yeast genomes
405   (Supplementary Table 7). For example, hardly any reductions are observed in PI4,5P2 binding
406   proteins (Slm1, Slm2 in *S. cerevisiae*[97]), which are involved in the regulation of actin
407   cytoskeleton organization and endosomal transport, or in class I myosins (myoA in *A.*
408   *nidulans*[98], myo5 in *S. cerevisiae*[99]) which are localized to the site of polarized growth and
409   involved in secretion and cell wall biogenesis.
410
411   Collectively, these data suggest that hyphal morphogenesis genes in general are
412   dispensable for yeasts to a smaller extent than genes with other functions. This is consistent
413   with most yeast-like fungi being able to switch to hyphal or pseudohyphal growth under certain
414   conditions. The fact that hyphal morphogenesis genes are not statistically significantly enriched
415   among losses compared to genome-wide expectation, however, is not in conflict with a
416   reduction of multicellular abilities in yeast-like fungi. These gene losses do indicate reductions in
417   hyphal growth, although this cutback is smaller compared to other functions in the genome. This
418   in turn suggests, that the ability for multicellular growth is among the functions preferentially
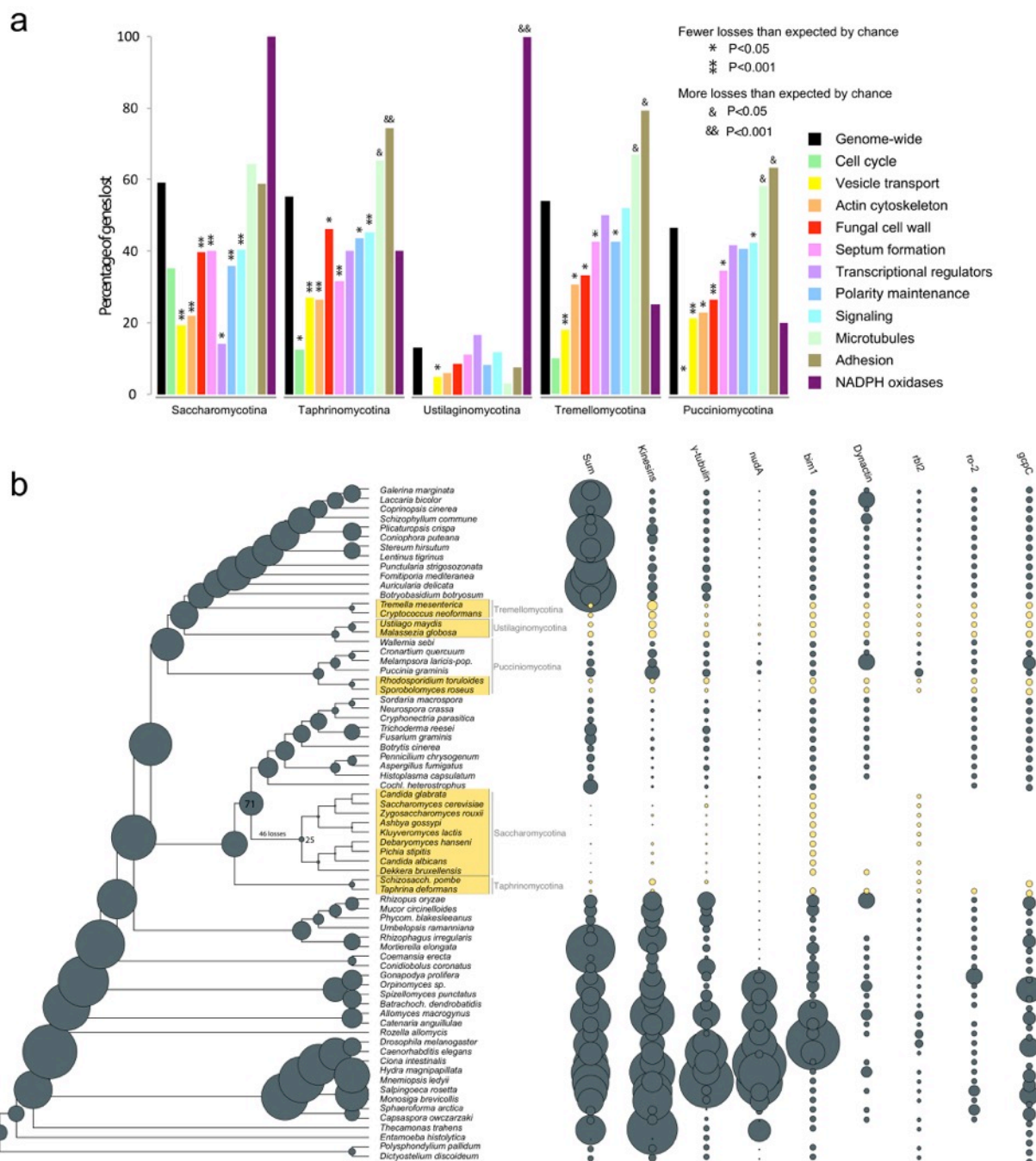419   retained by yeast-like fungi.

420
421 Fig. 6. Secondarily simplified yeast-like fungi retain genes for hyphal MC. (a) the percentages of lost
422 genes in main morphogenesis-related categories. Percentages were calculated relative to ancestral copy
423 numbers inferred in the node preceding the origin of 5 yeast-like clades (Saccharomycotina,
424 Taphrinomycotina, Pucciniomycotina, Ustilaginomycotina and Tremellomycotina). Significance of the
425 enrichment of gene losses in each category relative to genome-wide figures of gene loss were
426 determined by Fisher's exact test and is shown above bars. (b) ancestral gene copy number
427 reconstruction of microtubule-based transport genes along the fungal phylogeny. Secondarily simplified
428 (yeast-like) clades are highlighted in yellow. Bubble size proportional to reconstructed ancestral and
429 extant gene copy number across 19 gene families. Copy number distribution of each gene family is
430 shown right to the tree.

14

Conclusions

We analyzed the genetic underpinnings of the evolution of fungal hyphae. Hyphae are among the most enigmatic fungal structures with a unique multicellular organization, yet their evolutionary origins remained poorly explored. Our ancestral character state reconstructions localized the origin of hyphae to three nodes around the split of Blastocladio-, Chytridio- and Zoopagomycota (BCZ nodes), consistent with previous studies[17] and potential convergence of hypha-like structures in these phyla.

To understand how the underlying genetics evolved, we identified 362 gene families with known relevance to hyphal morphogenesis (e.g. from knockout studies) and predicted a link to hyphal MC for another 414 families using comparative genomics of 71 species. The evolutionary dynamics of these families shows a mixed picture. A large proportion of families are conserved in all sampled eukaryotes and show very little or no copy number dynamics at all at the origin of multicellular fungi. A second category comprises gene families with a deep eukaryotic origin that show duplications coincident with the evolution of hyphae. However, no families were found that had statistically significantly elevated number of duplications in BCZ nodes, indicating limited evolutionary novelty in these nodes. In the third category there are gene families whose origin mapped to BCZ nodes (RGSs, formins, APSES and Bem1 families). Such gene families could have evolved *de novo* or diverged in sequence so much that similarity is not detectable to homologous non-fungal sequences. We find candidates for both scenarios. For example, the MedA or APSES families contain fungal-specific protein domains; these have conceivably evolved in early fungi and represent fungal-specific innovations. On the other hand, the detected formin and RGS families contained only fungal genes, but their characteristic Interpro domains occur outside of fungi too, possibly reflecting common ancestry, with evidence for homology blurred by sequence divergence.

We found that several multicellularity-related genes predate the emergence of hyphal MC and were co-opted for hyphal growth during evolution, which mirrors patterns observed in multicellular animals and plants[6,100,101]. Such observations rise to the hypothesis that in terms of genetic novelty, transitions to multicellularity represent a minor rather than a major evolutionary step[102], an idea that finds support in the observations made here on fungi. Cell polarity maintenance, vesicle trafficking and cytoskeletal systems of unicellular eukaryotes may have turned out to be useful functions in hyphal MC, on which the extreme polarized growth of fungal hyphae could have built during evolution. The phagocytotic machinery was probably exapted for hyphal MC: its original function was most likely lifted by the emergence of a rigid cell wall in early fungi, which probably made the underlying genes dispensable. However, instead of being lost over time, its components got incorporated into hyphal MC.

Finally, beyond gene family events, certainly other genetic mechanisms (e.g. changes in amino acid sequence and domain composition, changes to biophysical properties of genes) also contributed to the evolution of hyphae. Our analyses of gene architecture revealed significant differences between MC-related genes of unicellular and multicellular fungi, indicating that changes in CDS length or intron content are also relevant for the emergence of hyphal MC[103].

15

474   Reports of sequence-level changes and domain shuffling in connection with the evolution of
475   hyphal MC have also been published. There is evidence for fungal kinesins being 2x more
476   processive than other eukaryotic kinesins[104] - probably in response to needs of long range
477   transport along the hyphal axis. Similarly, class V and VII chitin synthases gained a myosin
478   motor domain in early fungi, providing higher efficiency in polarized chitin synthesis[105–107].
479
480   Taken together, our results suggest that multiple mechanisms probably contributed to
481   the evolution of hyphal MC, including changes in gene structure, gene duplications, *de novo*
482   gene family birth, and co-option/neofunctionalization. Compared to other multicellular lineages,
483   the evolution of fungi shows several unique patterns. While the expansion of adhesion and
484   signal transduction mechanisms is shared by most colonial and aggregative multicellular
485   lineages examined so far[3,9,19,108–110], we did not find evidence for this in fungi. This could be
486   explained by the peculiar life history of fungal hyphae, which shares similarity with only
487   Oomycota. While adhesion might not be key in vegetative hyphae, there is plenty of evidence
488   for active communication between neighboring hyphae[111–113]. It is possible that the main modes
489   of communication in fungal hyphae are not linked to cell surface receptors, might be related to
490   volatiles (such as farnesol[80,114,115]) or are not known yet. These observations suggest that
491   multicellularity in fungi differs considerably from that in other lineages and raises the possibility
492   that hyphal MC should be considered a third, qualitatively different way in addition to the
493   aggregative and clonal modes of evolving MC. Subjective categorizations aside, hyphal MC
494   represents a highly successful adaptation to terrestrial life and comparative genomics opens the
495   door for discussions on whether major phenotypic transitions represent - in terms of genetic
496   novelty - a major or a minor transition.
497

498   Methods

499   **Organismal phylogeny**
500   We assembled a dataset containing whole proteomes of 71 species and performed all-vs-all
501   blast using mpiBLAST 1.6.0[116]. We omitted Microsporidia from the dataset due to the high rate
502   of evolution of this group. Proteins were clustered into gene families with Markov Cluster
503   Algorithm (MCL)[117] with an inflation parameter of 2.0. Clusters with at least 50% taxon
504   occupancy were chosen and were aligned by PRANK 140603[118] while trimAl 1.4.rev15[119] was
505   used to remove poorly aligned regions from the multiple sequence alignments using the
506   parameter –gt 0.2. Approximately-maximum-likelihood gene trees were inferred by FastTree[120]
507   using the LG+CAT model (-lg -cat20), and the option -gamma to compute a Gamma20-based
508   likelihoods. Using a custom-made Perl script we excluded gene trees with deep paralogs to
509   identify single-copy genes. Alignments of single-copy gene clusters were concatenated into a
510   supermatrix and a species tree was estimated using RAxML 8.2.4[121] under the
511   PROTGAMMAWAG model. The model was partitioned by gene. Bootstrapping was performed
512   on the dataset in 100 replicates.
513
514   **Ancestral character state reconstructions**

515   The 71 species were coded for their ability to form hyphae, either as hyphal or non-hyphal.
516   Species that could not be unambiguously assigned to hyphal or non-hyphal (*Catenaria*
517   *anguillulae*) and those with the ability to grow either as hyphae or unicells (most yeasts) were
518   coded as uncertain. Bayesian MCMC reconstruction of ancestral character states was
519   performed under the threshold model[122] using Bayesian MCMC with the "ancThresh" function in
520   phytools v0.6-60[123] in R[124]. The number of generations for MCMC was set to 1,000,000, and the
521   method "mcmc" was used with the Brownian motion as the model for the evolution of the
522   liability. Burn-in parameter was set to default. Convergence was checked by inspecting
523   likelihood values through time.
524
525   **Analyses of Gene family evolution**
526   To investigate the evolutionary dynamics of gene families containing hyphal morphogenesis-
527   related genes, we performed all-vs-all blast (NCBI Blast 2.7.1+)[125] for proteomes of the 71
528   species and did sequence similarity-based protein clustering by following the MCL clustering
529   protocol[117] used by Ohm et al 2012[126]. The resulting protein clusters were aligned by PRANK
530   140603[118] with default parameters, and ambiguously aligned regions were removed using trimAl
531   1.4.rev15[119] with the argument –gt 0.2. MAFFT v7.222[127] (option –-auto) was used as an
532   alternative alignment tool for clusters that could not be aligned by PRANK due to computational
533   limitations (80 out of 34032 clusters). Maximum Likelihood inference of gene trees and
534   calculation of Shimodaira-Hasegawa-like branch support values were carried out in RAxML
535   8.2.4[128] under the PROTGAMMAWAG model of protein evolution. The calculated SH-like
536   branch support values were used in gene tree-species tree reconciliation in Notung-2.9[129]. An
537   edge-weight threshold of 0.9 was used, as SH-like support values are usually less conservative
538   than ML bootstrap values (where 70% is usually taken as indication of strong support).
539   Reconciliation was performed on the maximum likelihood gene trees and the ML species tree
540   for the 71 species as input. We reconstructed the gene duplication/loss dynamics of gene
541   families along the species tree using respective scripts from the COMPARE pipeline[94,130]. The
542   numbers of gains and losses for each gene family and for each branch of the species tree were
543   recorded and mapped on the species tree. Ancestral gene copy numbers were calculated for
544   every internal node, summing the mapped duplications and losses across the species tree.
545   Mappings were generated for each of the functional groups and also for kinases, adhesion-
546   related proteins, receptors as well as for all gene families across the 71 genomes.
547
548   To test if genes related to hyphal MC experience an episode of increased duplication
549   rate in nodes where hyphal growth putatively originated (BCZ nodes), we performed gene
550   duplication enrichment analysis for each of the 362 families and for functional groups. To test if
551   a cluster or a functional group shows significantly more or less duplications than expected by
552   chance in BCZ nodes, we run two-tailed Fisher's exact tests ($p < 0.05$). We compared the
553   number of duplications mapped to BCZ nodes for a given gene family to the genome-wide
554   number of duplications in BCZ nodes, using total number of duplications across the tree as a
555   reference.
556
557   **Analyses of key multicellularity-related genes**

558 The above strategy was used to reconstruct the evolution of kinase, receptor and adhesion-
559 related gene families. Protein clusters containing kinase genes, both serine-threonine kinases
560 and histidine kinases, were collected based on InterPro domains. Identification of serine-
561 threonine kinases and histidine kinases followed Park et al 2011[131] and Herivaux et al 2016[88],
562 respectively. Classification of histidine kinases followed Defosse et al[87].
563
564 Families of adhesive proteins were identified based on experimentally characterized
565 genes collected from the literature. We identified 45 genes, which mostly grouped into
566 flocculins, lectins, hydrophobins and other (GPI)-modified cell wall adhesins. We identified
567 receptor genes based on InterPro domains that are annotated with the gene ontology term
568 'receptor activity' (but not 'receptor binding' or other terms indicative of indirect relationships to
569 receptor function), resulting in 27 IPR terms (IPR000161, IPR000276, IPR000337, IPR000363,
570 IPR000366, IPR000481, IPR000832, IPR000848, IPR001103, IPR001105, IPR001499,
571 IPR001546, IPR001946, IPR002011, IPR002185, IPR002280, IPR002455, IPR002456,
572 IPR003110, IPR003292, IPR003980, IPR003982, IPR005386, IPR006211, IPR017978,
573 IPR017979, IPR017981).
574

575 **Analyses of phagocytosis-related genes**
576 We collected information on phagocytosis-related genes from recent reviews on
577 *Dictyostelium*[65,66], identified the corresponding genes of this species in our dataset and the
578 protein clusters that contained homologs of the identified genes. Mapping of gene duplications
579 and losses along the species tree was done as described above.
580

581 **Genome-wide screen for putative hyphal multicellularity-related gene families**
582 To identify gene families with increased rates of gene duplication coinciding with the origin of
583 hyphal MC, we set up a pipeline that tests for higher than expected rate of duplication in nodes
584 of the species tree to which the origin of hyphae could be located (BCZ nodes). For each gene
585 family, gene duplication rates in BCZ nodes were compared to duplication rates of the same
586 family in other parts of the species tree (nodes before and after BCZ nodes). Gene duplication
587 rates were computed by dividing the number of reconstructed duplications for a given branch by
588 the length of that branch using a custom Perl script. Terminal duplications and duplications
589 mapped to metazoan ancestors were excluded from the analysis. The resulting
590 node×duplication rate matrix was analyzed by a two-factor permutation ANOVA[132] with degrees
591 of freedom DFT=2, in R, with $P < 0.05$ considered as significant. We further required that the
592 detected clusters be conserved (>=1 copy) in at least 70% of filamentous fungi.
593

594 **Analyses of gene losses in yeast-like fungi**
595 We analyzed gene losses in five yeast-like lineages by comparing the number of losses
596 genome-wide, to the numbers of losses in hyphal morphogenesis related genes (actin
597 cytoskeleton regulation, polarity maintenance, cell wall biogenesis/remodelling, septation and
598 septal plugging, signal transduction, transcriptional regulation, vesicle transport, microtubule-
599 based transport and cell cycle regulation) relative to ancestral copy numbers. P-values were
600 calculated by Fisher's exact test, with $P < 0.05$ considered as significant. The percentage of
601 genes retained in yeast genomes was calculated for every functional category by comparing

602 ancient gene-copy number prior to the emergence of yeast-like lineages to the average gene
603 copy-number of terminals.
604

605 **Statistical analysis of genomic features**
606 An R script (available upon request) was written to generate coding sequence (CDS)/intron
607 statistics (strand, order, length, count) based on genome annotations of the 71 species. CDS
608 feature coordinates for each gene were extracted and subsequently used to calculate intron
609 coordinates. Statistical significance of the differences between the gene, CDS and intron
610 lengths of 4 unicellular and 39 multicellular fungi was investigated by independent two-tailed
611 Welch's t-test with pooled variance estimation (var.equal=FALSE), using the t.test function in R.

Data availability

613 Files associated with this paper (including gene and species trees, gene duplication/loss
614 catalogs) have been deposited in Dryad (Accession number, *to be provided upon publication*).

Acknowledgements

Author contributions

625 E.K. and N.G.L. concieved the study. E.K. collected literature data on morphogenesis-related
626 genes. E.K. and A.N.P. inferred species trees, B.B. performed clustering, E.K., K.K., T.K., Z.M.
627 and T.V. analyzed gene family evolution. B.H. analyzed gene structural changes. E.K., M.R.,
628 N.T. and N.G.L. interpreted the results and wrote the paper. All authors have read and
629 commented on the manuscript.

Competing interests

631 The authors declare no competing interests.

References

633 1.   Szathmáry, E. Toward major evolutionary transitions theory 2.0. *Proc. Natl. Acad. Sci. U.*
634   *S. A.* **112,** 10104–11 (2015).
635 2.   Rokas, A. The Origins of Multicellularity and the Early History of the Genetic Toolkit For

636   Animal Development. *Annu. Rev. Genet.* **42,** 235–251 (2008).

637   3.   Abedin, M. & King, N. Diverse evolutionary paths to cell adhesion. *Trends Cell Biol.* **20,**
638   734–42 (2010).

639   4.   Coates, J. C., Aiman, U.-E. & Charrier, B. Understanding "green" multicellularity:
640   do seaweeds hold the key? *Front. Plant Sci.* **5,** 737 (2015).

641   5.   Brunet, T. & King, N. The Origin of Animal Multicellularity and Cell Differentiation. *Dev*
642   *Cell* **43,** 124–140 (2017).

643   6.   Sebé-Pedrós, A., Degnan, B. M. & Ruiz-Trillo, I. The origin of Metazoa: a unicellular
644   perspective. *Nat. Rev. Genet.* **18,** 498–512 (2017).

645   7.   Nagy, L. G., Kovács, G. M. & Krizsán, K. Complex multicellularity in fungi: evolutionary
646   convergence, single origin, or both? *Biol. Rev.* (2018). doi:10.1111/brv.12418

647   8.   Brown, M. W., Spiegel, F. W. & Silberman, J. D. Phylogeny of the "Forgotten"
648   Cellular Slime Mold, Fonticula alba, Reveals a Key Evolutionary Branch within
649   Opisthokonta. *Mol. Biol. Evol.* **26,** 2699–2709 (2009).

650   9.   Sebé-Pedrós, A. *et al.* Regulated aggregative multicellularity in a close unicellular relative
651   of metazoa. *Elife* **2,** e01287 (2013).

652   10.   Glöckner, G. *et al.* The multicellularity genes of dictyostelid social amoebas. *Nat.*
653   *Commun.* **7,** 12085 (2016).

654   11.   Ruiz-Trillo, I. *et al.* The origins of multicellularity: a multi-taxon genome initiative. *Trends*
655   *Genet.* **23,** 113–118 (2007).

656   12.   Fairclough, S. R. *et al.* Premetazoan genome evolution and the regulation of cell
657   differentiation in the choanoflagellate Salpingoeca rosetta. *Genome Biol.* **14,** R15 (2013).

658   13.   Blackwell, M. The Fungi: 1, 2, 3 … 5.1 million species? *Am. J. Bot.* **98,** 426–438 (2011).

659   14.   Niklas, K. J. & Newman, S. A. The origins of multicellular organisms. *Evol. Dev.* **15,** 41–
660   52 (2013).

661   15.   Harris, S. D. Branching of fungal hyphae: regulation, mechanisms and comparison with
662   other branching systems. *Mycologia* **100,** 823–832 (2008).

663   16.   Stajich, J. E. *et al.* The Fungi. *Curr. Biol.* **19,** R840–R845 (2009).

664   17.   Dee, J. M., Mollicone, M., Longcore, J. E., Roberson, R. W. & Berbee, M. L. Cytology and
665   molecular phylogenetics of Monoblepharidomycetes provide evidence for multiple
666   independent origins of the hyphal habit in the Fungi. *Mycologia* **107,** 710–728 (2015).

667   18.   Nagy, L. G. *et al.* Six Key Traits of Fungi: Their Evolutionary Origins and Genetic Bases.
668   in *The Fungal Kingdom* **5,** 35–56 (American Society of Microbiology, 2017).

669   19.   Sebé-Pedrós, A., Degnan, B. M. & Ruiz-Trillo, I. The origin of Metazoa: A unicellular
670   perspective. *Nature Reviews Genetics* **18,** 498–512 (2017).

671   20.   Svedberg, J. *et al.* Convergent evolution of complex genomic rearrangements in two
672   fungal meiotic drive elements. *Nat. Commun.* **9,** 4242 (2018).

673   21.   Fricker, M. D., Heaton, L. L. M., Jones, N. S. & Boddy, L. The Mycelium as a Network.
674   *Microbiol. Spectr.* **5,** (2017).

675   22.   Richards, T. A., Leonard, G. & Wideman, J. G. What Defines the "Kingdom"
676   Fungi? *Microbiol. Spectr.* **5,** (2017).

677   23.   Sekimoto, S., Rochon, D., Long, J. E., Dee, J. M. & Berbee, M. L. A multigene phylogeny
678   of Olpidium and its implications for early fungal evolution. *BMC Evol. Biol.* **11,** 331 (2011).

679   24.   Ryan, O. *et al.* Global gene deletion analysis exploring yeast filamentous growth. *Science*
680   **337,** 1353–6 (2012).

681   25.   Stajich, J. E. *et al.* Insights into evolution of multicellular fungi from the assembled
682   chromosomes of the mushroom Coprinopsis cinerea (Coprinus cinereus). *Proc. Natl.*
683   *Acad. Sci. U. S. A.* **107,** 11889–94 (2010).

684   26.   Kües, U., Khonsuntia, W. & Subba, S. Complex fungi. *Fungal Biol. Rev.* **32,** 205–218
685   (2018).

686   27.   Pöggeler, S., Nowrousian, M., Teichert, I., Beier, A. & Kück, U. Fruiting-Body

687		Development in Ascomycetes. in *Physiology and Genetics* 1–56 (Springer International
688		Publishing, 2018). doi:10.1007/978-3-319-71740-1_1
689	28.	Knoll, A. H. The Multiple Origins of Complex Multicellularity. *Earth Planet. Sci.* **39,** 217–
690		239 (2011).
691	29.	Verstrepen, K. J., Reynolds, T. B. & Fink, G. R. Origins of variation in the fungal cell
692		surface. *Nat. Rev. Microbiol.* **2,** 533–540 (2004).
693	30.	King, N., Hittinger, C. T. & Carroll, S. B. Evolution of Key Cell Signaling and Adhesion
694		Protein Families Predates Animal Origins. *Science (80-.).* **301,** 361–363 (2003).
695	31.	Miller, W. T. Tyrosine kinase signaling and the emergence of multicellularity. *Biochim.*
696		*Biophys. Acta - Mol. Cell Res.* **1823,** 1053–1057 (2012).
697	32.	Mendoza, A. de *et al.* Transcription factor evolution in eukaryotes and the assembly of
698		the regulatory toolkit in multicellular lineages. *Proc. Natl. Acad. Sci.* **110,** E4858–E4866
699		(2013).
700	33.	Harris, S. D. *et al.* Polarisome meets spitzenkörper: microscopy, genetics, and genomics
701		converge. *Eukaryot. Cell* **4,** 225–9 (2005).
702	34.	Steinberg, G. Hyphal growth: a tale of motors, lipids, and the Spitzenkörper. *Eukaryot.*
703		*Cell* **6,** 351–60 (2007).
704	35.	Sudbery, P. E. Regulation of polarised growth in fungi. *Fungal Biol. Rev.* **22,** 44–55
705		(2008).
706	36.	Harris, S. D. *et al.* Morphology and development in Aspergillus nidulans: A complex
707		puzzle. *Fungal Genet. Biol.* **46,** S82–S92 (2009).
708	37.	Steinberg, G., Peñalva, M. A., Riquelme, M., Wosten, H. & Harris, S. D. Cell Biology of
709		Hyphal Growth. *Microbiol. Spectr.* **5,** 1–34 (2017).
710	38.	Riquelme, M. *et al.* Fungal Morphogenesis, from the Polarized Growth of Hyphae to
711		Complex Reproduction and Infection Structures. *Microbiol. Mol. Biol. Rev.* **82,** e00068-17
712		(2018).
713	39.	Fischer, R., Zekert, N. & Takeshita, N. Polarized growth in fungi – interplay between the
714		cytoskeleton, positional markers and membrane domains. *Mol. Microbiol.* **68,** 813–826
715		(2008).
716	40.	Schultzhaus, Z. S. & Shaw, B. D. Endocytosis and exocytosis in hyphal growth. *Fungal*
717		*Biol. Rev.* **29,** 43–53 (2015).
718	41.	Schuster, M. *et al.* Co-delivery of cell-wall-forming enzymes in the same vesicle for
719		coordinated fungal cell wall formation. *Nat. Microbiol.* **1,** 16149 (2016).
720	42.	Momany, M. Polarity in filamentous fungi: establishment, maintenance and new axes.
721		*Curr. Opin. Microbiol.* **5,** 580–585 (2002).
722	43.	Virag, A. & Harris, S. D. The Spitzenkörper: a molecular perspective. *Mycol. Res.* **110,** 4–
723		13 (2006).
724	44.	Wendland, J. Comparison of Morphogenetic Networks of Filamentous Fungi and Yeast.
725		*Fungal Genet. Biol.* **34,** 63–82 (2001).
726	45.	Palecek, S. P., Kron, S. J. & Parikh, A. S. Sensing, signalling and integrating physical
727		processes during Saccharomyces cerevisiae invasive and filamentous growth.
728		*Microbiology* **148,** 893–907 (2002).
729	46.	Bahn, Y.-S. *et al.* Sensing the environment: lessons from fungi. *Nat. Rev. Microbiol.* **5,**
730		57–69 (2007).
731	47.	Biswas, S., Van Dijck, P. & Datta, A. Environmental sensing and signal transduction
732		pathways regulating morphopathogenic determinants of Candida albicans. *Microbiol. Mol.*
733		*Biol. Rev.* **71,** 348–76 (2007).
734	48.	Román, E., Arana, D. M., Nombela, C., Alonso-Monge, R. & Pla, J. MAP kinase
735		pathways as regulators of fungal virulence. *Trends Microbiol.* **15,** 181–190 (2007).
736	49.	Sudbery, P. E. Growth of Candida albicans hyphae. *Nat. Rev. Microbiol.* **9,** 737–748
737		(2011).

738   50.   Berbee, M. L., James, T. Y. & Strullu-Derrien, C. Early Diverging Fungi: Diversity and
739   Impact at the Dawn of Terrestrial Life. *Annu. Rev. Microbiol.* **71,** 41–60 (2017).
740   51.   Strullu-Derrien, C. *et al.* New insights into the evolutionary history of Fungi from a 407 Ma
741   Blastocladiomycota fossil showing a complex hyphal thallus. *Philos. Trans. R. Soc. B*
742   *Biol. Sci.* **373,** 20160502 (2018).
743   52.   Redecker, D., Kodner, R. & Graham, L. E. Glomalean fungi from the Ordovician. *Science*
744   **289,** 1920–1 (2000).
745   53.   Harris, S. D. Hyphal morphogenesis: an evolutionary perspective. *Fungal Biol.* **115,** 475–
746   484 (2011).
747   54.   Powell, M. J. Blastocladiomycota. in *Handbook of the Protists* 1497–1521 (Springer
748   International Publishing, 2017). doi:10.1007/978-3-319-28149-0_17
749   55.   Chang, Y. *et al.* Phylogenomic Analyses Indicate that Early Fungi Evolved Digesting Cell
750   Walls of Algal Ancestors of Land Plants. *Genome Biol. Evol.* **7,** 1590–1601 (2015).
751   56.   Spatafora, J. W. *et al.* The Fungal Tree of Life: From Molecular Systematics to Genome-
752   Scale Phylogenies. in *The Fungal Kingdom* **5,** 3–34 (American Society of Microbiology,
753   2017).
754   57.   Ahrendt, S. R. *et al.* Leveraging single-cell genomics to expand the fungal tree of life. *Nat.*
755   *Microbiol.* **3,** 1417–1428 (2018).
756   58.   Spatafora, J. W. *et al.* A phylum-level phylogenetic classification of zygomycete fungi
757   based on genome-scale data. *Mycologia* **108,** 1028–1046 (2016).
758   59.   Gravelat, F. N. *et al. Aspergillus fumigatus* MedA governs adherence, host cell
759   interactions and virulence. *Cell. Microbiol.* **12,** 473–488 (2010).
760   60.   Zhao, Y. *et al.* The APSES family proteins in fungi: Characterizations, evolution and
761   functions. *Fungal Genet. Biol.* **81,** 271–280 (2015).
762   61.   Lichius, A., Yáñez-Gutiérrez, M. E., Read, N. D. & Castro-Longoria, E. Comparative Live-
763   Cell Imaging Analyses of SPA-2, BUD-6 and BNI-1 in Neurospora crassa Reveal Novel
764   Features of the Filamentous Fungal Polarisome. *PLoS One* **7,** e30372 (2012).
765   62.   Bender, A. & Pringle, J. R. Use of a screen for synthetic lethal and multicopy suppressee
766   mutants to identify two new genes involved in morphogenesis in Saccharomyces
767   cerevisiae. *Mol. Cell. Biol.* **11,** 1295–305 (1991).
768   63.   Madden, K. & Snyder, M. CELL POLARITY AND MORPHOGENESIS IN BUDDING
769   YEAST. *Annu. Rev. Microbiol.* **52,** 687–744 (1998).
770   64.   Fujita, A. *et al.* Rax1, a protein required for the establishment of the bipolar budding
771   pattern in yeast. *Gene* **327,** 161–169 (2004).
772   65.   Bozzaro, S., Bucci, C. & Steinert, M. Chapter 6 Phagocytosis and Host–Pathogen
773   Interactions in Dictyostelium with a Look at Macrophages. in *International review of cell*
774   *and molecular biology* **271,** 253–300 (2008).
775   66.   Rivero, F. Endocytosis and the Actin Cytoskeleton in Dictyostelium discoideum. *Int. Rev.*
776   *Cell Mol. Biol.* **267,** 343–397 (2008).
777   67.   Mao, Y. & Finnemann, S. C. Regulation of phagocytosis by Rho GTPases. *Small*
778   *GTPases* **6,** 89 (2015).
779   68.   May, R. C., Caron, E., Hall, A. & Machesky, L. M. Involvement of the Arp2/3 complex in
780   phagocytosis mediated by FcγR or CR3. *Nat. Cell Biol.* **2,** 246–248 (2000).
781   69.   Epp, E. *et al.* Forward genetics in *Candida albicans* that reveals the Arp2/3 complex is
782   required for hyphal formation, but not endocytosis. *Mol. Microbiol.* **75,** 1182–1198 (2010).
783   70.   Hope, H., Bogliolo, S., Arkowitz, R. A. & Bassilana, M. Activation of Rac1 by the Guanine
784   Nucleotide Exchange Factor Dck1 Is Required for Invasive Filamentous Growth in the
785   Pathogen *Candida albicans*. *Mol. Biol. Cell* **19,** 3638–3651 (2008).
786   71.   Torruella, G. *et al.* Global transcriptome analysis of the aphelid Paraphelidium tribonemae
787   supports the phagotrophic origin of fungi. *Commun. Biol.* **1,** 231 (2018).
788   72.   Kollmar, M., Lbik, D. & Enge, S. Evolution of the eukaryotic ARP2/3 activators of the

WASP family: WASP, WAVE, WASH, and WHAMM, and the proposed new family members WAWH and WAML. *BMC Res. Notes* **5,** 88 (2012).

73. Chen, T. *et al.* Multigenerational Cortical Inheritance of the Rax2 Protein in Orienting Polarity and Division in Yeast. *Science (80-.).* **290,** 1975–1978 (2000).

74. Gonia, S. *et al.* Rax2 is important for directional establishment of growth sites, but not for reorientation of growth axes, during Candida albicans hyphal morphogenesis. *Fungal Genet. Biol.* **56,** 116–24 (2013).

75. Choi, E., Lee, K. & Song, K. Function of rax2p in the polarized growth of fission yeast. *Mol. Cells* **22,** 146–53 (2006).

76. Borkovich, K. A. *et al.* Lessons from the genome sequence of Neurospora crassa: tracing the path from genomic blueprint to multicellular organism. *Microbiol. Mol. Biol. Rev.* **68,** 1–108 (2004).

77. Corrochano, L. M. *et al.* Expansion of Signal Transduction Pathways in Fungi by Extensive Genome Duplication. *Curr. Biol.* **26,** 1577–1584 (2016).

78. Basu, R. & Chang, F. Characterization of Dip1p Reveals a Switch in Arp2/3-Dependent Actin Assembly for Fission Yeast Endocytosis. *Curr. Biol.* **21,** 905–916 (2011).

79. Wagner, A. R., Luan, Q., Liu, S.-L. & Nolen, B. J. Dip1 defines a class of Arp2/3 complex activators that function without preformed actin filaments. *Curr. Biol.* **23,** 1990–8 (2013).

80. Nickerson, K. W., Atkin, A. L. & Hornby, J. M. Quorum Sensing in Dimorphic Fungi: Farnesol and Beyond. *Appl. Environ. Microbiol.* **72,** 3805–3813 (2006).

81. Beaulieu, J. M. & O'Meara, B. C. Detecting Hidden Diversification Shifts in Models of Trait-Dependent Speciation and Extinction. *Syst. Biol.* **65,** 583–601 (2016).

82. Richards, T. A. & Talbot, N. J. Osmotrophy. *Curr. Biol.* **28,** R1179–R1180 (2018).

83. Lim, W. A. & Pawson, T. Phosphotyrosine Signaling: Evolving a New Cellular Communication System. *Cell* **142,** 661–667 (2010).

84. Suga, H. *et al.* Genomic survey of premetazoans shows deep conservation of cytoplasmic tyrosine kinases and multiple radiations of receptor tyrosine kinases. *Sci. Signal.* **5,** (2012).

85. de Mendoza, A., Sebé-Pedrós, A. & Ruiz-Trillo, I. The Evolution of the GPCR Signaling System in Eukaryotes: Modularity, Conservation, and the Transition to Metazoan Multicellularity. *Genome Biol. Evol.* **6,** 606–619 (2014).

86. Krizsan, K. *et al.* Transcriptomic atlas of mushroom development highlights an independent origin of complex multicellularity. *bioRxiv* 349894 (2018). doi:10.1101/349894

87. Defosse, T. A. *et al.* Hybrid histidine kinases in pathogenic fungi. *Mol. Microbiol.* **95,** 914–924 (2015).

88. Hérivaux, A. *et al.* Major Sensing Proteins in Pathogenic Fungi: The Hybrid Histidine Kinase Family. *PLOS Pathog.* **12,** e1005683 (2016).

89. Kirk, D. L. A twelve-step program for evolving multicellularity and a division of labor. *BioEssays* **27,** 299–310 (2005).

90. Wang, L., Zhai, B. & Lin, X. The Link between Morphotype Transition and Virulence in Cryptococcus neoformans. *PLoS Pathog.* **8,** e1002765 (2012).

91. Kempf, M. *et al.* Disruption of the GPI Protein-Encoding Gene IFF4 of Candida albicans Results in Decreased Adherence and Virulence. *Mycopathologia* **168,** 73–77 (2009).

92. Moreno-Ruiz, E. *et al.* The GPI-modified proteins Pga59 and Pga62 of Candida albicans are required for cell wall integrity. *Microbiology* **155,** 2004–2020 (2009).

93. Nagy, L. G. Evolution: Complex Multicellular Life with 5,500 Genes. *Curr. Biol.* **27,** R609–R612

94. Nagy, L. G. *et al.* Latent homology and convergent regulatory evolution underlies the repeated emergence of yeasts. *Nat. Commun.* **5,** 4471 (2014).

95. Shen, X.-X. *et al.* Tempo and Mode of Genome Evolution in the Budding Yeast

840   Subphylum. *Cell* **175,** 1533–1545.e20 (2018).

841   96.   Vierula, P. J. & Mais, J. M. A gene required for nuclear migration in Neurospora crassa
842   codes for a protein with cysteine-rich, LIM/RING-like domains. *Mol. Microbiol.* **24,** 331–40
843   (1997).

844   97.   Fadri, M., Daquinag, A., Wang, S., Xue, T. & Kunz, J. The Pleckstrin Homology Domain
845   Proteins Slm1 and Slm2 Are Required for Actin Cytoskeleton Organization in Yeast and
846   Bind Phosphatidylinositol-4,5-Bisphosphate and TORC2. *Mol. Biol. Cell* **16,** 1883–1900
847   (2005).

848   98.   McGoldrick, C. A., Gruver, C. & May, G. S. myoA of Aspergillus nidulans encodes an
849   essential myosin I required for secretion and polarized growth. *J. Cell Biol.* **128,** 577–87
850   (1995).

851   99.   Goodson, H. V, Anderson, B. L., Warrick, H. M., Pon, L. A. & Spudich, J. A. Synthetic
852   lethality screen identifies a novel yeast myosin I gene (MYO5): myosin I proteins are
853   required for polarization of the actin cytoskeleton. *J. Cell Biol.* **133,** 1277–91 (1996).

854   100.   Prochnik, S. E. *et al.* Genomic analysis of organismal complexity in the multicellular green
855   alga volvox carteri. *Science (80-.).* **329,** 223–226 (2010).

856   101.   Richter, D. J., Fozouni, P., Eisen, M. B. & King, N. Gene family innovation, conservation
857   and loss on the animal stem lineage. *Elife* **7,** (2018).

858   102.   Grosberg, R. K. & Strathmann, R. R. The Evolution of Multicellularity: A Minor Major
859   Transition? *Annu. Rev. Ecol. Evol. Syst.* **38,** 621–654 (2007).

860   103.   Lozada-Chávez, I., Stadler, P. F. & Prohaska, S. J. Genome-wide features of introns are
861   evolutionary decoupled among themselves and from genome size throughout Eukarya.
862   *bioRxiv* 283549 (2018). doi:10.1101/283549

863   104.   Lakämper, S., Kallipolitou, A., Woehlke, G., Schliwa, M. & Meyhöfer, E. Single fungal
864   kinesin motor molecules move processively along microtubules. *Biophys. J.* **84,** 1833–43
865   (2003).

866   105.   Fujiwara, M., Horiuchi, H., Ohta, A. & Takagi, M. A Novel Fungal Gene Encoding Chitin
867   Synthase with a Myosin Motor-like Domain. *Biochem. Biophys. Res. Commun.* **236,** 75–
868   78 (1997).

869   106.   Takeshita, N., Yamashita, S., Ohta, A. & Horiuchi, H. *Aspergillus nidulans* class V and VI
870   chitin synthases CsmA and CsmB, each with a myosin motor-like domain, perform
871   compensatory functions that are essential for hyphal tip growth. *Mol. Microbiol.* **59,** 1380–
872   1394 (2006).

873   107.   Sebé-Pedrós, A., Grau-Bové, X., Richards, T. A. & Ruiz-Trillo, I. Evolution and
874   Classification of Myosins, a Paneukaryotic Whole-Genome Approach. *Genome Biol. Evol.*
875   **6,** 290–305 (2014).

876   108.   Abedin, M. & King, N. The premetazoan ancestry of cadherins. *Science (80-.).* **319,** 946–
877   948 (2008).

878   109.   Niklas, K. J. & Newman, S. A. The origins of multicellular organisms. *Evol Dev* **15,** 41–52
879   (2013).

880   110.   Grau-Bove, X. *et al.* Dynamics of genomic innovation in the unicellular ancestry of
881   animals. *Elife* **6,** (2017).

882   111.   Dettmann, A., Heilig, Y., Valerius, O., Ludwig, S. & Seiler, S. Fungal Communication
883   Requires the MAK-2 Pathway Elements STE-20 and RAS-2, the NRC-1 Adapter STE-50
884   and the MAP Kinase Scaffold HAM-5. *PLoS Genet.* **10,** e1004762 (2014).

885   112.   Fischer, M. S., Wu, V. W., Lee, J. E., O'Malley, R. C. & Glass, N. L. Regulation of Cell-to-
886   Cell Communication and Cell Wall Integrity by a Network of MAP Kinase Pathways and
887   Transcription Factors in Neurospora crassa. *Genetics* **209,** 489–506 (2018).

888   113.   Serrano, A. *et al.* Spatio-temporal MAPK dynamics mediate cell behavior coordination
889   during fungal somatic cell fusion. *J. Cell Sci.* **131,** jcs.213462 (2018).

890   114.   Albuquerque, P. & Casadevall, A. Quorum sensing in fungi--a review. *Med. Mycol.* **50,**

891   337–45 (2012).

892   115.   Cottier, F. & Mühlschlegel, F. A. Communication in Fungi. *Int. J. Microbiol.* **2012,** 9
893   (2012).

894   116.   Darling, A. E., Carey, L. & Feng, W. The Design , Implementation , and Evaluation of
895   mpiBLAST. *Proc. Clust.* **2003,** 13–15 (2003).

896   117.   van Dongen, S. Graph clustering by flow simulation. *Graph Stimul. by flow Clust.* **PhD**
897   **thesis,** University of Utrecht (2000).

898   118.   Löytynoja, A. Phylogeny-aware alignment with PRANK. in 155–170 (Humana Press,
899   Totowa, NJ, 2014). doi:10.1007/978-1-62703-646-7_10

900   119.   Capella-Gutierrez, S., Silla-Martinez, J. M. & Gabaldon, T. trimAl: a tool for automated
901   alignment trimming in large-scale phylogenetic analyses. *Bioinformatics* **25,** 1972–1973
902   (2009).

903   120.   Price, M. N., Dehal, P. S. & Arkin, A. P. FastTree: Computing Large Minimum Evolution
904   Trees with Profiles instead of a Distance Matrix. *Mol. Biol. Evol.* **26,** 1641–1650 (2009).

905   121.   Stamatakis, A. RAxML-VI-HPC: maximum likelihood-based phylogenetic analyses with
906   thousands of taxa and mixed models. *Bioinformatics* **22,** 2688–2690 (2006).

907   122.   Felsenstein, J. A comparative method for both discrete and continuous characters using
908   the threshold model. *Am. Nat.* **179,** 145–56 (2012).

909   123.   Revell, L. J. ANCESTRAL CHARACTER ESTIMATION UNDER THE THRESHOLD
910   MODEL FROM QUANTITATIVE GENETICS. *Evolution (N. Y).* **68,** 743–759 (2014).

911   124.   Ihaka, R. & Gentleman, R. R: A Language for Data Analysis and Graphics. *J. Comput.*
912   *Graph. Stat.* **5,** 299–314 (1996).

913   125.   Camacho, C. *et al.* BLAST+: Architecture and applications. *BMC Bioinformatics* **10,** 1–9
914   (2009).

915   126.   Ohm, R. A. *et al.* Diverse Lifestyles and Strategies of Plant Pathogenesis Encoded in the
916   Genomes of Eighteen Dothideomycetes Fungi. *PLoS Pathog.* **8,** e1003037 (2012).

917   127.   Katoh, K., Misawa, K., Kuma, K. & Miyata, T. MAFFT: a novel method for rapid multiple
918   sequence alignment based on fast Fourier transform. *Nucleic Acids Res.* **30,** 3059–66
919   (2002).

920   128.   Stamatakis, A. RAxML version 8: A tool for phylogenetic analysis and post-analysis of
921   large phylogenies. *Bioinformatics* **30,** 1312–1313 (2014).

922   129.   Chen, K., Durand, D. & Farach-Colton, M. NOTUNG: A Program for Dating Gene
923   Duplications and Optimizing Gene Family Trees. *J. Comput. Biol.* **7,** 429–447 (2000).

924   130.   Nagy, L. G. *et al.* Comparative genomics of early-diverging mushroom-forming fungi
925   provides insights into the origins of lignocellulose decay capabilities. *Mol. Biol. Evol.* **33,**
926   959–970 (2016).

927   131.   Park, G. *et al.* Global Analysis of Serine-Threonine Protein Kinase Genes in Neurospora
928   crassa. *Eukaryot. Cell* **10,** 1553–1564 (2011).

929   132.   Nagy, L. G. *et al.* Genetic Bases of Fungal White Rot Wood Decay Predicted by
930   Phylogenomic Analysis of Correlated Gene-Phenotype Evolution. *Mol. Biol. Evol.* **34,** 35–
931   44 (2017).

932
933
934
935
936
937
938
939
940
941

942

Supplementary Figures

943

945 For

Comparative genomics reveals the origin of hyphae and
multicellularity

947

948

950 Enikő Kiss, Botond Hegedüs, Torda Varga, Zsolt Merényi, Tamás Kószó, Balázs Bálint, Arun N.
951 Prasanna, Meritxell Riquelme, Norio Takeshita, László G. Nagy

Contents:

985

986
987

988   Supplementary Figure 1. Phylogenetic age distribution of hypha morphogenesis genes. Figure
989   mirrors main text Figure 2 with gene names provided for each dot.
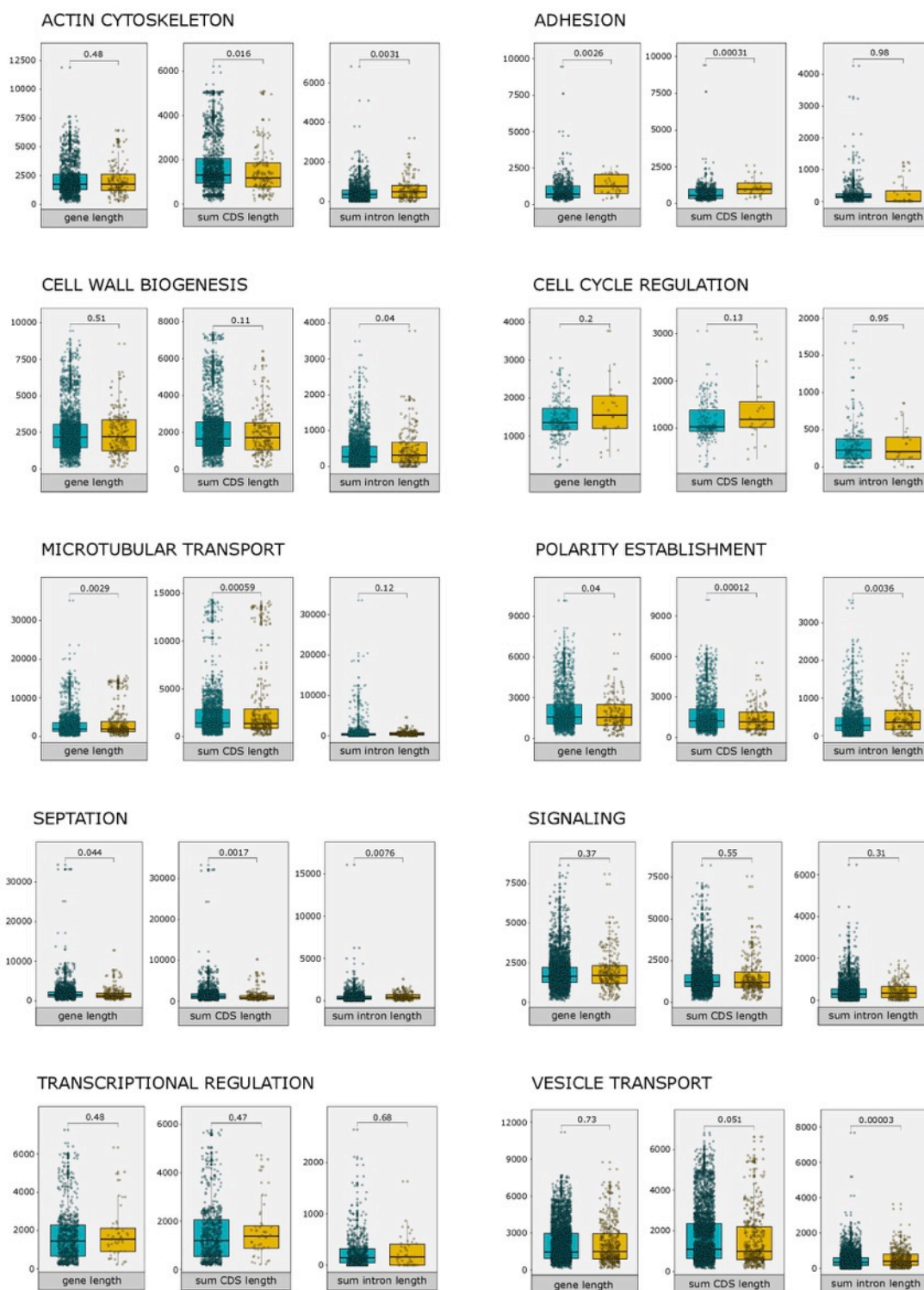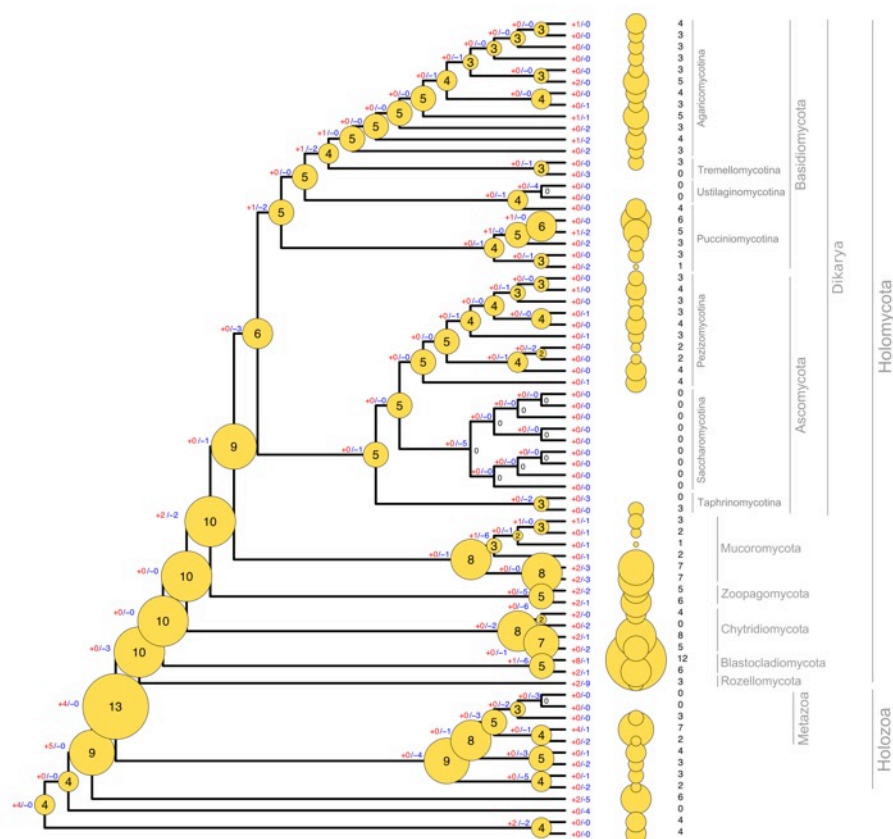
990
991
992
993
994
995
996
997
998
999

1000

1001 Supplementary Figure 2. Statistical comparisons of basic structural properties of genes related
1002 to hyphal MC. Box plots display differences in gene, CDS and intron lengths of 4 unicellular
1003 (yellow) and 39 multicellular fungi (blue) in nine functional categories.
1004

1005
1006 Supplementary Figure 3. Reconstructions of ancestral gene copy numbers of histidine-kinase
1007 genes. Numbers at the branches represent gene duplications (+) and losses (-) inferred by
1008 COMPARE. Bubble size is proportional to reconstructed ancestral gene copy number. Copy
1009 number distribution for each species is shown right to the tree.
1010
1011
1012
1013
1014
1015
1016
1017
1018
1019
1020
1021
1022

1023
1024 Supplementary Fig. 4. Reconstructions of ancestral gene copy numbers of NADPH-oxidase
1025 genes. Numbers at the branches represent gene duplications (+) and losses (-) inferred by
1026 COMPARE. Bubble size is proportional to reconstructed ancestral gene copy number. Copy
1027 number distribution for each species is shown right to the tree.
1028
1029